Synthesis and Characterization of Surface-Protected Nanocrystalline Titania Particles

Emmanuel Scolan and Clément Sanchez*

Laboratoire de Chimie de la Matière Condensée, UMR CNRS 7574, Université Pierre et Marie Curie, 4 place Jussieu, 75252 Paris Cedex 05, France

Received May 1, 1998. Revised Manuscript Received July 14, 1998

Monodisperse nonaggregated nanoparticles of titania are obtained through hydrolysis at 60 °C of titanium butoxide in the presence of acetylacetone and para-toluenesulfonic acid. After the particles are dried, the resulting xerosols can be dispersed without aggregation in water−alcoholic or alcoholic solutions at concentrations higher than 1 M. The characterizations of the nanoparticles were carried out in solution by using quasi-elastic light scattering (QELS); FTIR; ^{13}C, ^{17}O, and ^{1}H NMR and in solid state by X-ray diffraction, transmission electron microscopy (TEM), FTIR, thermogravimetry−dynamic thermal analysis (TG−DTA), ^{13}C cross-polarization−magic angle spinning (CP−MAS) NMR. The mean size of the anatase oxide core can be adjusted in the 1−5 nm range by a careful tuning of the synthetic conditions. The protection of these particles toward aggregation is ensured through the complexation of the surface by acetylacetonato ligands and through an adsorbed hybrid organic−inorganic layer made with acetylacetone, para-toluenesulfonic acid, and water.

Introduction

Sol−gel processes are a way to make dispersed materials through the growth of metal oxo-polymers in a solvent.[1,2] The chemistry involved in sol−gel processes is based on hydrolysis and condensation reactions of metallo-organic compounds such as metal alkoxides ($M(OR)_n$). The structure and the morphology of the resulting network strongly depend on the relative contribution of each of these reactions. The combination of these metal oxo-polymers can produce bushy structures which invade the whole volume, forming gels when these oxo-polymers reach macroscopic sizes.[1,3] Indeed a gel is not the only possible outcome for such polymerization reactions. Other final states may be reached, including sols when the polymerized structures did not reach macroscopic sizes, and precipitates when the reactions produce dense structures rather than bushy ones.[3] This variability comes from the many different ways in which oligomers and polymers can be linked and organized when they are dispersed in a solvent.

For transition metal alkoxide precursors, the major problem is to control hydrolysis−condensation rates which are generally too fast, resulting in the formation of precipitates with a high degree of microstructural disorder.[2] An attractive strategy is to use hydroxylated strong complexing ligands (SCL) such as carboxylic acids, β-diketones, and allied derivatives which modify the reactivity of the precursors.[4−10] Indeed, many transparent sols and gels made of transition metal-oxo-polymers have been obtained by hydrolyzing complexed metal alkoxides. However, even if the resulting oxo-oligomers or oxo-polymers are generally polydisperse in size and composition,[10] they correspond to metastable amorphous states that exhibit a very high surface-to-volume ratio making them prone to high chemical reactivity and partial reversibility.[11] As a consequence these sols can be used as a reservoir of reactive matter which can be recombined to produce crystalline phases. A careful tuning of the experimental conditions (initial hydrolysis ratio $H = [H_2O]/[M]$, complexing ratio $A = [SCL]/[M]$, temperature, acidity $H^+ = [H^+]/[M]$, solvent) allows one to obtain crystalline transition metal oxide based nanoparticles.[9] Recently, sol−gel synthesis of nanocrystalline titanium dioxide and templated amorphous titanium dioxide were explored by many research groups.[12−16] Applications of titanium dioxide colloids

* To whom correspondence should be addressed. Phone: +33 1 44 27 55 34. Fax: +33 1 44 27 67 49. E-mail: clems@ccr.jussieu.fr.

(1) Brinker, C. J.; Scherrer, G., Eds. *Sol−Gel Science: The Physics and Chemistry of Sol−Gel Processing*, ed. Academic Press: San Diego, CA, 1990.
(2) Livage, J.; Henry, M.; Sanchez, C. *Prog. Solid State Chem.* **1988**, *288*, 259.
(3) Kallala, M.; Sanchez, C.; Cabane, B. *Phys. Rev. E.* **1993**, *48*, 3692.
(4) Sanchez, C.; Livage, J.; Henry, M.; Babonneau, F. *J. Non-Cryst. Solids* **1988**, *100*, 65.
(5) Debsikbar, J. C. *J. Non-Cryst. Solids* **1986**, *87*, 343.
(6) Léaustic, A.; Babonneau, F.; Livage, J. *J. Non-Cryst. Solids* **1989**, *1*, 248.
(7) Ribot, F.; Toledano, P.; Sanchez, C. *Chem. Mater.* **1991**, *3*, 759.
(8) Papet, P.; Lebars, N.; Baumard, J. F.; Lecomte, A.; Dauger, A. *J. Mater. Sci.* **1989**, *24*, 3850.
(9) Chatry, M.; Henry, M.; In, M.; Sanchez, C.; Livage, J. *J. Sol-Gel Sci. Technol.* **1994**, *1*, 233.
(10) Blanchard, J.; Barboux-Dœuff, S.; Maquet, J.; Sanchez, C. *New J. Chem.* **1995**, *19*, 929.
(11) Blanchard, J.; Schaudel, B.; In, M.; Sanchez, C. *Eur. J. Inorg. Chem.* **1998**, *8* (4), 985.
(12) Kumar, K.-N. P.; Keizer, K.; Burggraaf, A. J.; Okubo, T.; Nagamoto, H.; Morooka, S. *Nature* **1992**, *358*, 48.
(13) O'Regan, B.; Grätzel, M. *Nature* **1991**, *353*, 737.
(14) (a) Antonelli, D. M.; Ying, J. Y. *Angew. Chem., Int. Ed. Engl.* **1995**, *34*, 2014. (b) Stathatos, E.; Lianos, P.; Del Monte, F.; Levy, D.; Tsourvas, D. *Langmuir* **1997**, *13*, 4295.
(15) Moritz, T.; Reiss, J.; Diesner, K.; Su, D.; Chemseddine, A. *J. Phys. Chem. B* **1997**, *101*, 8052.

10.1021/cm980322q CCC: $15.00
Published on Web 09/24/1998

and thin films are numerous, including photovoltaic, electrochromic, photochromic, electroluminescence, and catalytic devices and sensors.[16]

The work described in the present article combines all the above-mentioned strategies.[8−11] This article describes the synthesis of monodisperse nonaggregated particles of titania for which mean size can be adjusted in the 1−5 nm range. Moreover, after the particles are dried, the resulting xerosols can be dispersed without aggregation in water−alcoholic or alcoholic solutions, thus improving the processability of these nanomaterials. The characterizations of these titania nanoparticles are performed both in solution and in the solid state by using quasi-elastic light scattering (QELS); FTIR; ^{13}C, ^{17}O, and ^{1}H NMR, and X-ray diffraction (XRD), transmission electron microscopy (TEM), FTIR, thermogravimetry-differential thermal analysis (TG−DTA), and ^{13}C cross-polarization−magic angle spinning (CP−MAS) NMR, respectively.

Experimental Section

Materials. All experiments were performed under atmospheric conditions. All products were purchased from Fluka except butan-1-ol (SdS) and 10% ^{17}O-enriched water (Isotec), and were used without further purification.

Preparation of the Sols S_A. To a solution of pentan-2,4-dione or acetylacetone (AcacH, the acetylacetonato ligand bound to titanium will be denominated Acac) in *n*-butanol, titanium *n*-butoxide ($Ti(OBu^n)_4$) was added slowly and the mixture was stirred at room temperature for 15 min. An exothermic reaction occurred which led to a yellow solution. Hydrolysis of the clear mixture was then performed by the dropwise addition of an aqueous acidic solution (para-toluenesulfonic acid (PTSH), $HClO_4$, or HNO_3). The resulting aged solution acidified with PTSH exhibits a pH of 2.3 ± 0.1 his solution was then heated overnight at 60 °C giving rise to transparent sols which remain stable for several months. The pH of the resulting sols is of about 1.1 ± 0.1. The different parameters are defined as

$$\text{initial complexant/metal ratio:} \quad A = \frac{[\text{Acac}]}{[\text{Ti}]}, \quad 1 \le A \le 6$$

$$\text{initial hydrolysis ratio:} \quad H = \frac{[H_2O]}{[\text{Ti}]}, \quad 5 \le H \le 10$$

$$\text{acidity ratio:} \quad H^+ = \frac{[H^+]}{[\text{Ti}]}, \quad 0 \le H^+ \le 0.8$$

The typical concentration of titanium in the sol ranges from 0.5 to 1 M. In the following article standard sols (variable A, H = 10, H^+ (PTSH) = 0.2) were particularly studied and labeled as S_A sol.

Preparation of the Xerosols X_A. the dried xerosols X_A were obtained after ultracentrifugation or solvent evaporation of the S_A sol. The drying procedure was performed under vacuum at room temperature or by heating at 100 °C.

The xerosols can be dispersed in alcoholic or water−alcoholic solutions at concentrations higher than 1 M in titanium. The resulting sols were made of nonaggregated nanoparticles as checked by QELS and TEM.

Techniques. The dynamic QELS distributions were obtained on an AMTEC SM200 spectrogoniometer with a He/Ne laser (λ = 632.8 nm) and interfaced with a Bi2030AT Brookhaven photocorrelator.

TEM observations were performed using a JEOL 100 CXII (100 kV) microscope. A drop of the sols was deposited onto a carbon-coated grid.

FTIR spectra were recorded on a Nicolet Magna 550 spectrometer (32 scans at a resolution of 4 cm^{-1}). Attenuated total reflection (ATR) technique was used for the sols. The xerosol samples were pelleted with dried KBr.

Simultaneous TG−DTA analyses were carried out using a Netzsch STA/QMS-System 409/429-403 with a heating rate of 5 °C min^{-1} under a flow of 75 cm^3 min^{-1} of air/argon. The TGA measurements were coupled with a mass spectrometer.

The XRD patterns were obtained with a Philips PW1830 powder diffractometer operating in reflection geometry with Cu Kα radiation (λ = 1.5406 Å) and equipped with a graphite back monochromator. The patterns were recorded over the 2θ range from 10 to 80° with a 2θ step size of 0.05° and a scanning rate of 40 s per step. The position and width of the $K_{\alpha 1}$ lines were determined using the fit profile subroutine of the Philips APD 3.5 program package. The average particle size was deduced from the half-height line broadening by applying the Scherrer formula assuming Gaussian profiles for experimental and instrumental broadenings.

^{13}C CP-MAS solid-state NMR spectra were recorded on a Bruker MSL400 spectrometer at 100.62 MHz. The samples were spun at 4 kHz using a zirconium oxide 4 mm rotor. All of the CP experiments were performed under Hartmann−Hahn match condition,[17] which was carefully set and periodically checked (T_{90° (^1H) = 6 μs). Isotropic chemical shifts are referenced to tetramethylsilane (TMS). The ^{13}C CP-MAS NMR spectra were recorded with 10 different contact times (T_{CP}) from 0.05 ms up to 15 ms. The recycle delay between pulses was 10 s. The number of scans was 1000 for each CP experiment.

The spectra were simulated and the signal intensities determined with the WIN-FIT program.[18] Intensity values were plotted as a function of the contact time and simulated with two conventionally accepted models for describing the spin dynamic associated with CP experiments.[19] The simplest model applies to spins that are partially decoupled from the protons such as quaternary carbons.[20,21] The second model concerns spins that are dipolar coupled, such as CH or CH_2.[22,23] The behavior of CH_3 groups is more complex because of the fast internal rotation that partially averages the effect of the dipolar coupling. It was fitted by using the second model which was reported to give satisfying quantitative results.[24]

^{13}C and ^{1}H in solution NMR spectra were recorded using a Bruker AC300 spectrometer operating at 75.47 MHz for ^{13}C and 300.13 MHz for ^{1}H. Because ^{17}O has a low natural abundance (0.037%), ^{17}O-enriched water (10% in weight) was used for the synthesis of the sample. The ^{17}O NMR spectra of ^{17}O-enriched titanium oxo-polymers have been previously reported.[10] They are characterized by four broad bands which can be unambiguously assigned to oxo-bridges (μ_2-O, μ_3-O), Acac species, and water, on the basis of the published literature.[10,25,26] ^{17}O NMR spectra in solution were recorded using a Bruker MSL400 spectrometer operating at 54.22 MHz for ^{17}O. C_6D_6 was used as lock solvent as external standard (δ_H = 7.16 ppm; δ_C = 128.4 ppm (triplet of benzene)).

(16) Gerfin, T.; Grätzel, M.; Walder, L. *Molecular and Supramolecular Surface Modification of Nanocrystalline TiO_2 Films: Charge-Separating and Charge-Injecting Devices*; Gerfin, T., Grätzel, M., Walder, L., Eds.; John Wiley and Sons: New York, 1997; Vol. 44.

(17) Hartmann, S. R.; Hahn, E. L. *Phys. Rev.* **1962**, *128*, 2042.

(18) Massiot, D.; Thiele, H.; Germanus, A. *Bruker Rep.* **1994**, *140*, 43.

(19) Sangill, R.; Rastrup-Andersen, N.; Bildsoe, H.; Jakobsen, H. J.; Nielsen, N. C. *J. Magn. Res.* **1994**, *A107*, 67.

(20) Pines, A.; Gibby, M. G.; Waugh, J. S. *Chem. Phys.* **1973**, *59*, 569.

(21) Müller, L.; Kumar, A.; Baumann, T.; Ernst, R. R. *Phys. Rev. Lett.* **1974**, *32*, 1402.

(22) Alemany, L. B.; Grant, D. M.; Pugmire, R. J.; Alger, T. D.; Zilm, K. W. *J. Am. Chem. Soc.* **1983**, *105*, 6697.

(23) Wu, X.; Zilm, K. W. *J. Magn. Res.* **1993**, *A102*, 205.

(24) Babonneau, F.; Maquet, J.; Bonhomme, C.; Richter, R.; Röwer, G.; Bahloul, D. *Chem. Mater.* **1996**, *8*, 1415.

(25) Day, V. W.; Eberspacher, T. A.; Klemperer, W. G.; Park, C. W.; Rosenberg, F. S. *J. Am. Chem. Soc.* **1991**, *113*, 8190.

(26) Day, V. W.; Eberspacher, T. A.; Klemperer, W. G.; Park, C. W. *J. Am. Chem. Soc.* **1993**, *115*, 8469.

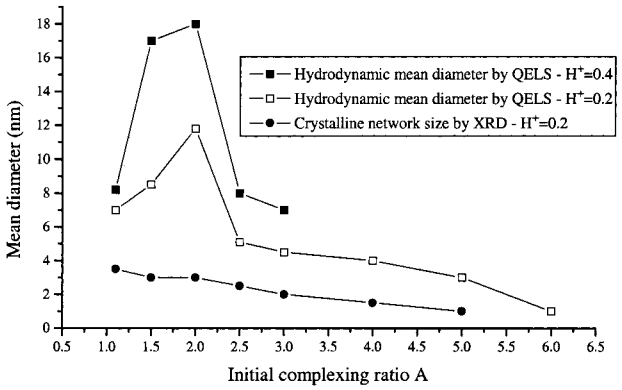

Figure 1. Evolution of the mean diameter measured by QELS (■) and (□) or deduced from the half-height line broadening on X-ray diffractograms (●) for sols or xerosols respectively prepared with different acidity ratios H^+ (PTSH), initial complexing ratios A and $H = 10$.

pH measurements were performed on the sols at the different stages of the process by using a Metrohm 718 STAT Titrino potentiometer and a combined Mettler pH electrode which enables pH to be measured at temperatures up to 100 °C. The pH setup was calibrated at several temperatures between 25 and 60 °C, with buffer solutions (pH = 4 and 7). The pH was compared with butanol−water−acetylacetone solutions, the compositions of which were close to that of the solvent composing the sols, which contained different amounts of PTSH.

Results and Discussion

Characterization of the Sols. *QELS.* QELS experiments were performed on different room temperature synthesized sols before they were heated at 60 °C. Sols synthesized without acid gave bimodal distributions with mean hydrodynamic diameters located at about 7 and 50 nm. Room temperature synthesized sols made with acid produced a particle size of about 2 nm. In all cases broad size distributions were generally observed for the resulting colloidal particles or aggregates.

The influence of four parameters (the different ratios A, H, and H^+ defined in the Experimental Section and the nature of the anion of the acid) on the size of particles in clear sols was studied. For $H = 5$ (A = 1 and H^+ (PTSH) = 0.2), a precipitate is formed, whereas a clear sol was obtained for $H = 10$. It seems that a large excess of water is favorable to sol stability. This excess should increase the dielectric constant of the solvent sufficiently to favor ionic dissociation and solvation. The use of HNO_3 or $HClO_4$ ($H^+ = 0.2$, $H = 10$) leads to clear sols only for initial complexation ratios above $A = 3$ and 4, respectively. However, in these sols aggregation of the titanium oxo-particles cannot be fully avoided as shown by the relatively large measured mean hydrodynamic diameters (10−25 nm). After sols are heated, in acidic medium (PTSH) quite monodisperse size distributions are observed for S_A sols. The evolutions of the particle sizes measured by QELS are reported in Figure 1. The analysis of these data shows that sols are made of nanometric colloidal particles, the mean diameter of which increases when A decreases or H^+ increases. Better control of the synthetic conditions and better adjustment of the mean diameters were obtained with PTSH and for $H^+ = 0.2$. In these cases,

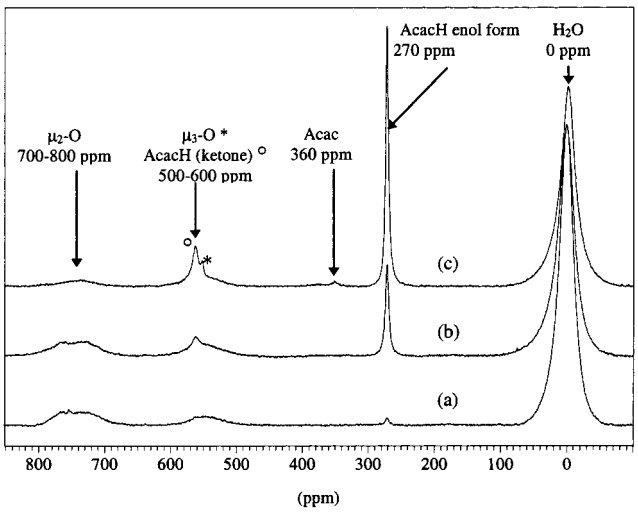

Figure 2. ^{17}O NMR spectra of sols (a) sol S_1 (A = 1, $H = 10$, H^+(PTSH) = 0.2; aging at $T = 20$ °C for 10 min, no heating); (b) sol S_1 (A = 1, $H = 10$, H^+(PTSH) = 0.2; aging at $T = 20$ °C for 4 h, no heating); (c) sol S_1 (A = 1, $H = 10$, H^+(PTSH) = 0.2; aging at $T = 60$ °C overnight).

QELS measurements exhibit a quite monodisperse size distribution. The mean hydrodynamic diameter ranges from 7 to 1.5 nm when the complexing ratio A is increased from 1 to 5. Afterward, S_A sols (A, $H = 10$, H^+ (PTSH) = 0.2) were studied, in particular.

FTIR Spectroscopy. Infrared spectra of all the S_A sols show strong vibration bands at 1600 and 1530 cm^{-1} (ν_{C-O} and $\nu_{C=C}$ respectively) characteristic of the enol-form of acetylacetonato groups bonded to titanium. They display also the bands corresponding to the acetylacetone free in solution, namely the bands at 1725, 1705 (ν_s(C═O), and ν_a(C═O), respectively, of the ketonic form), and 1620 cm^{-1} (ν_{C-O} and $\nu_{C=C}$, respectively, of the enolic form). In the sol state, the amount of free AcacH and Acac bonded to titanium is of the same order of magnitude as that determined through the intensity of the FTIR bands. However, a quantitative analysis of the ratio between bonded and free ligands by IR is not straightforward. This ratio will be determined by NMR and chemical analysis (vide infra).

After the sol is dried, the IR spectra recorded on the corresponding xerosols do not exhibit the bands characteristic of free AcacH, showing that mainly all of the remaining acetylacetone molecules are bonded to titanium atoms.

NMR in Solution. The ^{17}O, ^{13}C, and ^1H NMR spectra in solution of the sols were recorded for different complexing ratio (A ranges from 1 to 5).

Typical ^{17}O solution NMR spectra recorded for sols are reported before (figures 2a and 2b) and after (Figure 2c) heating sol S_1 at 60 °C. They exhibit the characteristic ^{17}O NMR resonances of water (0 ppm), AcacH (enolic form at 275 ppm, ketonic form at 565 ppm) and many weak resonances around 750, 550 (oxygens belonging to μ_2-O and μ_3-O bridges respectively), and 360 ppm (Acac bonded to titanium).[10] After the sol is heated at 60 °C the resonances corresponding to acetylacetone (free AcacH and bound Acac) increase because the enrichment process occurring through the cetol intermediates is enhanced.[11] Moreover, the intensity of the resonances corresponding to the μ_2−O bridges decreases

Table 1. ^{13}C NMR Data of PTSH Species: Sol S_1, Sol S_4, PTSH in Butanol/AcacH/Water Solution, and PTS^-Na^+ in Butanol/AcacH/Water Solution

	δ_{C-S} (ppm)	δ_{C-CH3} (ppm)	δ_{CH} (ppm)	δ_{CH} (ppm)	δ_{CH3} (ppm)
S_4	143.7	140.7	129.5	127.1	21.7
S_1	142.9	141.0	129.6	127.1	21.7
PTSH	142.7	141.1	129.7	126.9	21.6
$PTS^- Na^+$	142.5	141.2	129.7	126.9	21.6

while a sharp resonance located at 556 ppm corresponding to μ_3−O bridges starts to appear. This well-defined ^{17}O NMR resonance could probably arise from μ_3−O bulk species, as are those reported for crystalline titanium oxo-compounds (for anatase $\delta_{\mu3-O} = 561$ ppm, for many titanium oxo cluster $\delta_{\mu3-O}$ ranges between 500 and 570 ppm).[10,25−27]

The ^{13}C NMR spectra display the characteristic resonances of free species in solution. As an example for the S_1 sol, these resonances are the following locations: at for free AcacH $\delta_{CH3} = 25.1/31.2$ ppm (enol/ketone), $\delta_{CH} = 101.2$ ppm (enol), $\delta_{CH2} = 58.7$ ppm (ketone), and $\delta_{C=O} = 192.7/205.4$ ppm (enol/ketone), and for butanol $\delta_{CH3} = 14.5$ ppm, and $\delta_{CH2} = 19.9/35.6$ ppm, and $\delta_{CH2OH} = 62.5$ ppm. Some broad resonances corresponding to bonded or adsorbed entities (Acac, butoxy) (for bound Acac $\delta_{CH3} = 26.5$ ppm, $\delta_{CH} = 105.2$ ppm, $\delta_{C=O} = 188.8$ ppm, and butoxy groups $\delta_{CH2OTi} = 77.5$ ppm) are also observed. However, they only correspond to a small amount of the "bonded" ligands. The main parts of the bound ligands are not observed in these NMR in solution experiments, because they are attached to titanium oxo-species or titanium oxo-polymers having a lower mobility than molecular species. This phenomenon generally increases relaxation times and thus broadens the NMR lines of the corresponding species whose characteristic resonances become unobservable.

It is interesting to point out that the chemical shift, line width, and intensity of the ^{13}C NMR resonances corresponding to the observed PTSH species strongly depend on the particle size. The ^{13}C NMR data are reported in Table 1, with those of reference samples recorded from solutions of PTS^- and PTSH in a solvent, the composition of which is very close to that of the reactional bath. As an example, the ^{13}C NMR resonances corresponding to the quaternary carbons of the aromatic ring of PTSH-derived species are shown in Figure 3. All of the resonances characteristic of the PTSH-derived species become sharper and strongly shift with respect to the position of free PTSH and PTS^- when the initial [AcacH]/[Ti] ratio increases, i.e., when the particle size decreases. This phenomenon seems characteristic of an exchange process. Taking into account the shift tendency observed for the resonances (Figure 3), this exchange cannot be due to an exchange process simply involving free PTSH and free PTS^-. This exchange probably involves free PTS^-/PTSH species and PTS^- molecules which experience stronger interactions with the nanoparticles. These latter will likely be bonded to the metal atoms or adsorbed in the solvation sphere of the titania particles. Adsorption behavior of sulfonates was already observed for zirconia nanoparticles made by sol−gel.[9] Titanium oxo-clusters and

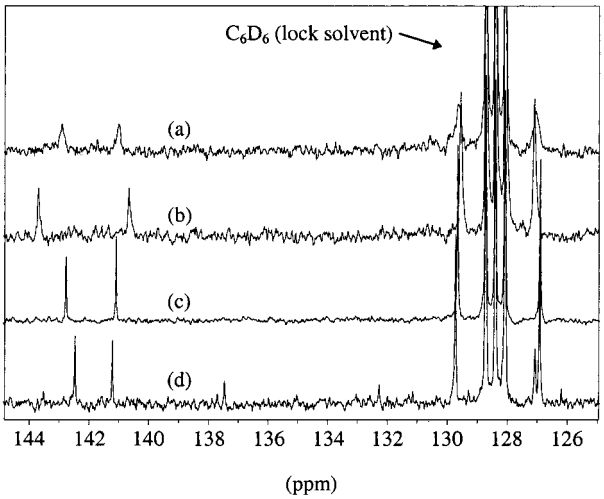

Figure 3. ^{13}C NMR spectra of the aromatic carbons of PTSH species: (a) sol S_1 ($A = 1$, $H = 10$, $H^+(PTSH) = 0.2$); (b) sol S_4 ($A = 4$, $H = 10$, $H^+(PTSH) = 0.2$); (c) PTSH in butanol/AcacH/water and solution; (d) PTS^- in butanol/AcacH/water solution.

titanium oxo-polymers in which sulfonate groups are apparently bonded to titanium even after hydrolysis have recently been reported by Schubert et al.[28]

The ^1H NMR spectra show characteristic signals corresponding to free butanol, AcacH, and PTSH in solution. In addition, some broad peaks assigned to bound species start to appear when the particle size decreases, but their integration is not quantitative. The quantitative integration of the peaks corresponding to free species in solution allows one to estimate by difference the relative amount of the different species (bound Acac, adsorbed PTS) interacting with the colloidal particles. The free butanol resonances were taken as an internal reference assuming that in the presence of a large amount of water and in acidic conditions mainly all butoxy groups have been released from the titanium coordination sphere. The estimated ratio between bound Acac and free AcacH ([Acac-Ti-surface]/[AcacH]) ranges typically at 0.3 for sols S_1 and S_4. This value is close to those reported for surface complexed of zirconia (0.43) and ceria (0.3) colloidal nanoparticles.[29,30] They correspond to the values observed at plateau in classical adsorption isotherms which are represented on the plot of the concentration of bound Acac by surface metal atom versus the concentration of free AcacH in solution.[29,30]

Using this semiquantitative approach, a mean raw formula can be estimated for the particles. It was found that

for sol S_1, $TiO_{1.9}(Acac)_{0.2}\cdot 1.80\ H_2O\cdot 0.09$ PTSH

for sol S_3, $TiO_{1.7}(Acac)_{0.6}\cdot 3.9\ H_2O\cdot 0.06$ PTSH

for sol S_4, $TiO_{1.6}(Acac)_{0.8}\cdot 5.3\ H_2O\cdot 0.05$ PTSH

(27) Bastow, T. J.; Stuart, S. N. *Chem. Phys.* **1990**, *143*, 459.

(28) Lorenz, A.; Kickelbick, G.; Schubert, U. *Chem. Mater.* **1997**, *9*, 2551.

(29) Peyre, V.; Spalla, O.; Belloni, L.; Nabavi, M. *J. Colloid Interface Sci.* **1997**, *187*, 184.

(30) Spalla, O.; Kékicheff, P. *J. Colloid Interface Sci.* **1997**, *192*, 43.

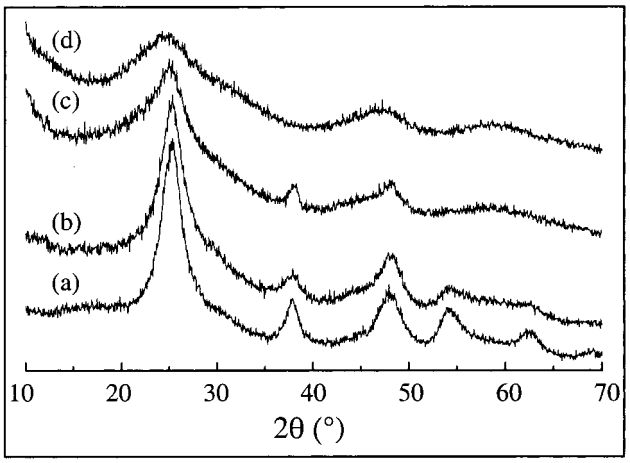

Figure 4. X-ray diffraction patterns of samples dried at 100 °C: (a) X_1, (b) X_3, (c) X_4, (d) X_1 without PTSH ($H^+ = 0$).

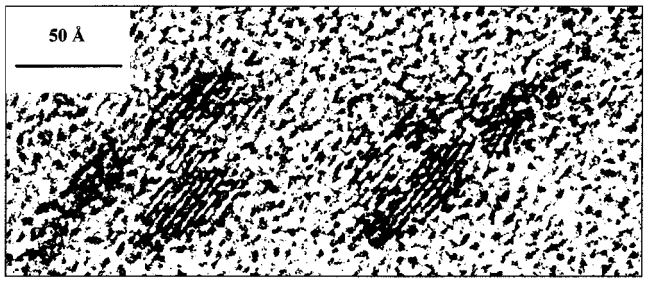

Figure 5. TEM images of anatase TiO_2 nanoparticles (S_1).

Clearly, the amount of estimated Acac bound to titanium increases from sol S_1 to sol S_4 in agreement with the fact that the particle size decreases (vide infra, XRD experiments) and thus the surface-to-volume ratio increases from sol S_1 to sol S_4. Both PTSH species and water are associated to the nanoparticles, and are probably located in the solvatation shell.

Characterizations of the Xerosols. *XRD−TEM.* Figure 4 shows the typical XRD patterns recorded for the xerosols. These patterns are characteristic of crystalline particles of TiO_2 anatase.[31] The mean size of the titania particles was fitted from the measured line width using the Debye relation assuming that the line broadening is essentially due to the size effect. The average sizes, deduced from the full width at half-maximum, are reported in Figure 1. When *A* increases the line width becomes broader and thus the particle size becomes smaller. The diffractogram of the sample made without PTSH exhibits no crystalline character. The calculated values for the particle size range between 40 Å for xerosol X_1 to 15 Å for xerosol X_4. These values are consistent with the mean sizes observed by TEM experiments which show the lattice planes of crystalline nanoparticles with a diameter of about 40 Å (see Figure 5). Moreover, electron diffraction performed on these particles shows that the oxide phase corresponds to crystalline titania anatase and the lattice planes to (101) orientation (d_{101} = 3.52 Å).[31] The different drying methods led to identical xerosols containing nanocrystalline anatase particles with the same mean diameter. The large difference between the sizes deduced from QELS experiments and those measured from XRD shows that a large amount of solvating or adsorbed species are belting the particles in solution.

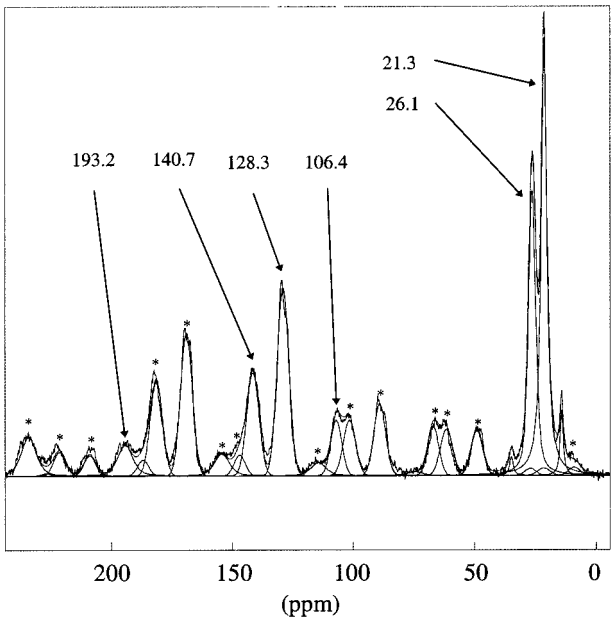

Figure 6. ^{13}C CP-MAS spectrum of xerosol X_1 (A = 1, H = 10, H^+(PTSH) = 0.2) (full bold line = experimental spectrum, simple line = simulation); T_{CP} = 3 ms, spinning rate = 4 kHz, 5968 scans; ∗ spinning sidebands.

TGA−DTA. From TGA data, the main metal oxide/organics ratio measured for xerosols is of about 60/40. Four mass losses are observed on TG traces. They should correspond to the elimination of hydration water (120 °C, 4% mass loss, endothermic), the release and combustion of bound or adsorbed organic species (220 °C, 7.7% mass loss, exothermic; 380 °C, 25.3% mass loss, exothermic), and to the transformation of anatase titania into the stable rutile form (around 600 °C, 3.7% mass loss), as suggested by XRD experiments performed on the calcinated samples (1000 °C). During the combustion of organics, the main molecules detected by mass spectrometry are water, CO_2, acetic acid, acetone, carbonates, SO_2, and SO_3. The formation of acetone and acetic acid results from the thermal decomposition process of acetylacetone catalyzed by Lewis acids such as titanium (retro Claisen reaction).[32,33]

^{13}C CP−MAS NMR. Xerosols were studied by ^{13}C CP−MAS NMR, including high-power decoupling. A ^{13}C CP−MAS NMR spectrum of xerosol X_1 is shown in Figure 6 and was measured for a contact time T_{CP} = 3 ms. The spectrum indicates the presence of four sets of isotropic lines around 20−30 ppm, 105 ppm, 125−145, and 190 ppm. The first lines located at 21.3 and 26.2 ppm are assigned to the methyl groups of Acac ligands and PTSH, respectively. The three other sets of resonances located at about 106.1, 128, and 140 ppm correspond to ^{13}CH of acetylacetonato ligands and to the resonances of CH groups and quaternary carbons of the aromatic ring of the PTSH moieties, respectively. The presence of anisotropic resonances located around 193.2 ppm are characteristic of ^{13}CO groups of the Acac

(31) Powder Diffraction File; J. C. P. D. S. International Center for Diffraction Data: Swarthmore, PA, 1993, no. 21−1272.

(32) Steunou, N. Ph.D. Thesis, Université Pierre et Marie Curie, Paris VI, 1997.

(33) Poncelet, O.; Hubert-Pfalzgraf, L. G. *Polyhedron* **1990**, *9*, 1305.

Table 2. Fitted Magnetization Values for ^{13}C CP−MAS NMR Resonances Recorded for Xerosol X_1 ($A = 1$, $H^+ = 0.2$, $H = 10$)

	resonance	magnetization intensity	normalized number of carbons for each molecule
	CH	12 568	4.3
PTSH	C	5016	1.8
	CH_3	3203	1.1
	CH	2631	1.0
AcacH	**C**=O	2742	1.0
	CH_3	5870	2.1

ligands. The characteristic resonances of free butanol and butoxy ligands are very weak and practically negligible. These results indicate that in the xerosols, PTSH and bound Acac are the two main organic species that remain on the particles after drying, while the cleavage of the butoxy groups is quasi-complete. The ratios between the two remaining organic species, i.e., the Acac ligands and the residual PTSH groups, were measured from the NMR data. However, it is well known that rapid internal molecular motion may lead to partial averaging of NMR interactions, which are anisotropic in nature. These interactions are essentially chemical shift anisotropy (CSA) and dipolar coupling (with ^1H) in the case of ^{13}C solid-state NMR spectroscopy. The CP behavior of the different nuclei can be markedly different for the various sites. Thus, it is not a straightforward matter to obtain quantitativity from only one ^{13}C CP−MAS NMR spectrum. ^{13}C CP−MAS NMR spectra were recorded with different contact times from 0.05 to 15 ms. As a consequence, quantitative ^{13}C CP−MAS NMR data were obtained by fitting all of the spectra resonances and their evolution for different contact times with the usual appropriate model.[24] The typical agreement obtained between experimental and simulated spectra is shown in Figure 6.

As an example, the values of the different fitted magnetic intensities are reported in the Table 2. The results show that for the X_1 xerosol the [Acac]/[PTSH] ratio is about 0.9. This ratio is in agreement with those obtained through elemental chemical analysis (0.83). The elemental analysis performed on the xerosol X_1 indicates that the S/Ti ratio is about 0.18 ± 0.02, which corresponds to the global [PTS species]/[Ti] ratio. By difference the carbon weight ratio gives a [Acac]/[Ti] ratio of about 0.15 ± 0.02. This result is also consistent with the calculated values deduced from the integration of the ^1H NMR spectra recorded in the sol state ([Acac]/[Ti] = 0.2). The smaller value obtained in the solid state probably results from the evaporation of some AcacH molecules.

The process of formation of these titania nanoparticles from complexed titanium alkoxides can be described as follows. For Acac complexed tetravalent metal alkoxides ($M(OR)_4$, M = Ti, Zr, Ce, Sn ...) in alcoholic solutions, the reaction bath contains a collection of oligomeric alkoxides, composed with reactive noncomplexed precursors $M(OR)_4$ and less reactive modified metal alkoxides $M(OR)_{4-x}(Acac)_x$ ($x = 0, 1, 2$) in equilibrium.[34] The concentration of the different species depends on the nature of the metal atom and on the initial complexing ratio A = [AcacH]/[M].[6,10] For titanium butoxide, the noncomplexed species are trimers and solvated oligomers and the complexed species are dimers $[Ti(OBu)_3(Acac)]_2$ and monomers $[Ti(OBu)_2(Acac)_2]$.[10] For $A \geq 1$ a mixture of complexed and uncomplexed precursors is obtained, but for $A \geq 2$ titanium 6-folded $[Ti(OBu)_2(Acac)_2]$ monomers are the main species present in solution.[10] Because the driving force of reactivity of titanium alkoxides toward nucleophilic species is related to the possibility of the metallic center to increase its coordination, complexed precursors that can easily reach a 6-fold coordination (as in TiO_2) exhibit a lower reactivity toward hydrolysis−condensation reactions. Moreover, the substitution of hydrolyzable butoxy groups by weakly hydrolyzable Acac ligands lowers the functionality of the precursors.[4,34]

In light of our experimental data, the hydrolysis−condensation behavior of complexed metal alkoxides can be explained as follows. Upon addition of water to the precursor, a series of chemical reactions occur (hydrolysis of butoxy groups, partial cleavage of some Acac−titanium bonds, condensations) which lead to the formation of $Ti_2O_2(Acac)_4$ dimers and amorphous titanium oxo-polymers. This was evidenced through ^{17}O NMR experiments.[10] In these conditions a typical NMR spectrum exhibits one sharp resonance corresponding to μ_2−O (750 ppm) and three broad resonances corresponding to μ_2−O (700−800 ppm), μ_3−O (500−600 ppm), and bound Acac (360 ppm) characteristic of $Ti_2O_2(Acac)_4$ and titanium oxo-polymers respectively.[10] The size of the titanium oxo-polymers, was analyzed by light scattering techniques. With a complexation range $A \geq 1$ hydrolysis of acetylacetone-modified precursors leads to sols with broadly distributed amorphous particles having a mean hydrodynamic diameter ranging from about 10 to 40 Å. Hydrolyzed and partially condensed species reach a metastable state in which growth is inhibited by the capping of the species by Acac ligands and residual butoxy groups located at the surface of the particles. These ligands inhibit the spatial extension of the metal oxo-network and prevent aggregation and precipitation. This synthesis method based on the competitive growth/termination mechanism of metal oxo-species in the presence of Acac surface capping agents, however, leads to the formation of xerosols which are amorphous by XRD.[10,34]

Such capping agents protect but also slow the possible rearrangements and collapse of the first obtained species (metal oxo-clusters, oxo-polymers). These rearrangements are needed for the formation of crystalline titania. It is well known that acidic conditions decrease the complexing power of the inhibitor ligand (Acac) and thus favor ligand exchange for reorganization.[35] Acidity, temperature, and high hydrolysis ratios tend also to speed the hydrolysis rates, leading to a fast cleavage of all the butoxy groups. Moreover, acidity induces an efficient protonation of the titanium oxo-bridges (zero charge point of TiO_2 = 6.5) promoting fast redissolution−precipitation reactions, and higher temperatures (60 °C) provide some thermal energy favoring the structural reorganizations needed for the crystallization of titania.

Therefore, the hydrolysis of Acac-modified titanium butoxide performed in the presence of PTSH followed

(34) Sanchez, C.; Ribot, F. *New J. Chem.* **1994**, *18*, 1007.

(35) Stumm, W.; Kummert, R.; Sigg, L. *Croat. Chem. Acta* **1980**, *53*, 291.

by an aging at 60 °C leads to the formation of nanocrystalline particles of titania.

In these conditions, for each preparation the ratio between surface bound Acac and free AcacH is practically constant (in all cases, the plateau corresponding to the classical adsorption isotherm is reached). Consequently any variation of the initial concentration of AcacH (A = [AcacH]/[Ti]) yields a variation of the possible amount of surface-adsorbed Acac species. Thus, because the growth of these crystalline particles is surface controlled, an increase of the *A* ratio yields to a decrease of the size of the oxide core; typically the core diameter decreases from 40 to 15 Å when *A* increases from 1 to 4.

The resulting titania nanoparticles are nonaggregated because they are surface capped with acetylacetonato ligands in equilibrium with free AcacH remaining in solution. Moreover, some PTSH-based species and some water molecules are located in a solvating layer surrounding the nanoparticles. These adsorbed species seem also to play a particular role in the stabilization. The amphiphilic character of PTSH species which can probably better accommodate the Acac capped surface, should be one reason of this specific behavior, because other hydrophilic inorganic anions such as ClO_4^- or NO_3^- known to have a different complexing power, do not provide such efficient results.

Conclusion

Monodisperse nanoparticles of titania are obtained through hydrolysis of acetylacetone-complexed titanium butoxide in the presence of protons. The mean size of the anatase oxide core can be adjusted in the 1−5 nm range. These nanoparticles are nonaggregated even for concentration higher than 1 M in titanium. The protection of these particles toward aggregation is ensured through the complexation of the surface by acetylacetonato ligands and through an adsorbed hybrid organic−inorganic layer made with acetylacetone, PTSH, and water. After the resulting xerosols are dried, they can be dispersed without aggregation in water−alcoholic or alcoholic of solutions, improving the processability of these nanomaterials.

Acknowledgment. We would like to acknowledge Jocelyne Maquet for her help in NMR measurements, Claude Magnier for his scientific interest on this study, and the French Ministery of Research and Rhone-Poulenc S.A. for the financial support.

CM980322Q